Research Article **Open Access**

Katarzyna Dołżyk-Szypcio*

Stress–dilatancy relationship for railway ballast

https://doi.org/10.2478/sgem-2018-0018
received March 23, 2018; accepted June 26, 2018.

Abstract: Knowledge of the mechanical behaviour of ballast is very important for designing a railway track, especially for high-speed lines. The monotonic drained triaxial tests of scaled and fouled ballast presented in literature were analysed using the Frictional State Theory. The stress–plastic dilatancy relationship shows that four characteristic stages of shearing may be specified. The influence of stress level and water content may be quantified by the use of the Frictional State Theory.

Keywords: railway ballast; critical state; frictional state; dilatancy.

1 Introduction

Railway transportation is a currently universal mode of transportation offering safety, energy efficiency and zero CO_2 emissions at the point of use. The track bed is constructed of layers above the natural ground for reducing the stresses induced by train passage. For construction of the highest layer of track bed, ballast is used. The thickness of the ballast layer is typically a minimum of 250–300 mm. Ballast is an unbounded coarse aggregate with particle size ranging between 22.5 mm and 63 mm [1]. Ballast should have resistance against crushing and attrition induced by repetitive loading as well as mechanical and weathering degradation. In time, grain modification in ballast gradation due to the processes of crushing, weathering and infiltration of material from the surface and underlying layer is observed [2].

The mechanical behaviour of ballast is very important to provide (predict) safety and economy of the rail track maintenance. Large-scale triaxial tests are usually curried out to study the mechanical behaviour of ballast under monotonic and repetitive loading [1-5]. These large-scale triaxial tests are very expensive. Some researchers (e.g. Aingaran [1]) have used a smaller triaxial apparatus for the testing of scaled ballast samples with 150 mm diameter and 300 mm height. The scaled ballast is a parallel gradation of the full-scale ballast but with particles that are about three times smaller.

The influence of the water content on the permanent deformation of unbounded materials was studied by Werkmeister et al. [5], Ekblad [6] and Trinh et al. [2]. The results show that the water content strongly reduces the resilient modulus and increase permanent deformation.

High values of the peak friction angle and the non-linear failure envelope at low normal stress are characteristic for ballast. This phenomenon is related to the interlocking of grains and the ability of ballast to dilate at low stress levels [1]. The values of the critical state parameter M for fresh and recycled ballast were approximately 1.90 (Φ_{cv}'=46.2°) and 1.67 (Φ_{cv}'=40.8°), respectively. The critical strength increases with increase of the confining pressure [4].

In this paper, the stress–dilatancy relationship of scaled and fouled ballast is analysed using the data from tests conducted by Aingaran [1] on scaled ballast samples with 150 mm diameter and 300 mm height, as well as the data provided by Trinh et al. [2], who conducted monotonic triaxial tests on ballast samples with 300 mm diameter and 600 mm height. The Frictional State Theory [7] is used for the analysis. The influence of stress level and water content on stress–dilatancy behaviour is shown.

2 Stress–Dilatancy Relationship

The stress–dilatancy relationship obtained from the Frictional State Theory [8] for drained triaxial tests has the following form:

$$\eta = Q - AD^p \tag{1}$$

where

$$\eta = q/p' \tag{2.a}$$

***Corresponding author: Katarzyna Dołżyk-Szypcio,** Faculty of Civil and Environmental Engineering, Bialystok University of Technology, Bialystok, Poland, E-mail: k.dolzyk@pb.edu.pl

$$Q = M^o - \alpha\, A^o \tag{2.b}$$

$$A = \beta\, A^o \tag{2.c}$$

$$M^o = \frac{6\sin\Phi^o}{3-\sin\Phi^o} \tag{2.d}$$

$$A^o = 1 - \frac{1}{3} M^o \tag{2.e}$$

$$q = \sigma_1^{'} - \sigma_3^{'} \tag{2.f}$$

$$p^{'} = \frac{1}{3}\left(\sigma_1^{'} + 2\sigma_3^{'}\right) \tag{2.g}$$

$$D^p = \frac{\delta\varepsilon_\upsilon^p}{\delta\varepsilon_q^p} \tag{2.h}$$

$$\delta\varepsilon_\upsilon^p = \delta\varepsilon_1^p + 2\delta\varepsilon_3^p \tag{2.i}$$

$$\delta\varepsilon_q^p = \frac{2}{3}\left(\delta\varepsilon_1^p - \delta\varepsilon_3^p\right) \tag{2.j}$$

Φ^o is the critical state friction angle, and α and β are the Frictional State Theory parameters.

The plastic parts of volumetric and shear strain increments are calculated from the following equations:

$$\delta\varepsilon_\upsilon^p = \delta\varepsilon_\upsilon - \delta\varepsilon_\upsilon^e \tag{3.a}$$

$$\delta\varepsilon_q^p = \delta\varepsilon_q - \delta\varepsilon_q^e \tag{3.b}$$

where

$$\delta\varepsilon_\upsilon^e = \frac{\delta p^{'}}{K} \tag{4.a}$$

$$\delta\varepsilon_q^e = \frac{\delta q}{3G} \tag{4.b}$$

In this paper, the parameter κ of Cam clay model and Poisson's ratio ν are used for calculation of the bulk and shear moduli from the following equations:

$$K = \frac{1}{2(1+\nu)}\,\frac{\vartheta\, p^{'}}{\kappa} \tag{5.a}$$

$$G = \frac{3(1-2\nu)}{2(1+\nu)}\,\frac{\vartheta\, p^{'}}{\kappa} \tag{5.b}$$

where the specific volume

$$\vartheta = 1 + e \tag{6}$$

and e is the void ratio.

In this paper, it is assumed that Poisson's ratio is independent of the void ratio and stress level, and that ν=0.3 for scaled ballast and ν=0.27 for fouled ballast. The κ values are calculated using Eq. (5.b) for $G \approx G_s$, where G_s is the secant shear modulus at the initial (quasi-elastic) stage of shearing:

$$G_s = \frac{\delta q}{3\delta\varepsilon_q} \tag{7}$$

The assumed values of κ and ν for scaled and fouled railway ballast for later calculation are shown in Tables 1 and 2, respectively.

Table 1: Experimental conditions and elastic parameters of scaled railway ballast.

σ_c [kPa]	w	e_o [–]	κ [–]	ν [–]
15	Dry	0.774	0.0027	0.30
25		0.801	0.0027	0.30
60		0.759	0.0027	0.30
115		0.771	0.0027	0.30
200		0.774	0.0027	0.30
15	Saturated	0.787	0.0027	0.30
20		0.781	0.0027	0.30

Table 2: Experimental conditions and elastic parameters of fouled railway ballast.

σ_c [kPa]	w	e_o [–]	κ [–]	ν [–]
30	4.0	0.350	0.0013	0.27
100	4.0	0.350	0.0015	0.27
200	4.0	0.350	0.0020	0.27
400	4.0	0.350	0.0030	0.27
100	12.0	0.350	0.0018	0.27
400	12.0	0.350	0.0045	0.27

3 Behaviour of Ballast During Drained Triaxial Shear

The characteristic stress–plastic dilatancy relationship for ballast during the conventional drained triaxial shear is shown in Figure 1.

At the initial stage (Stage I) of shearing ($0 \leq \varepsilon_a < 0.1$–0.15%), elastic and quasi-elastic behaviour is observed. Thus, theoretically, $\delta\varepsilon_\upsilon^{\,e}=\delta\varepsilon_\upsilon$ and $\delta\varepsilon_q^{\,e}=\delta\varepsilon_q$; so, $\delta\varepsilon_\upsilon^{\,p}=\delta\varepsilon_q^{\,p}=0$, and the plastic dilatancy D^p cannot be calculated. Highly unstable values of plastic dilatancy were obtained in this study. At this stage of shearing, the Frictional State Theory cannot be used. The point Y_1 represents the onset of Stage II of shearing, at which stable increments of volumetric and shear plastic strain suddenly appear. At this phase of shearing, the increments of mean normal stress ($\delta p'$) and shear stress (δq) grow quickly. So, the elastic parts of the volumetric and shear strain increments are considerable. Hence, at this stage of shearing, the plastic parts of volumetric and shear strain increments are also relatively large. For most of the analysed experimental data, plastic dilatancy at this stage is positive, and point Y_2 – representing the compression during shear – does not reach the transitional point where the sample starts to dilate. At this stage, the value of the secant shear modulus decreases quickly. The stress ratio–plastic dilatancy (η–D^p) relationship is almost linear, and the parameters α_1 and β_1 of the Frictional State Theory can be computed for assumed value of the critical frictional state angle Φ°.

The point Y_2 represents the onset of Stage III of shearing, during which the elastic parts of the strain increments ($\delta\varepsilon_\upsilon^{\,e}$, $\delta\varepsilon_q^{\,e}$) are small or very small compared to the global (plastic) strain increments. At this stage of shearing, the secant shear modulus is small and decreases to zero at the peak point named F ('failure point'). The relation η–D^p is linear, so the parameters α_2 and β_2 may be simply computed. Stage IV, namely, the post-peak behaviour of the ballast is generally unstable, but for the analysed experimental data, the relation η–D^p may be approximated by a straight line, and the parameters α_3 and β_3 may be computed. Generally, at the peak, the shear band is formed and non-homogeneous deformation of the sample is observed. The classical shear band has not been observed by Aingaran [1] and Trinh et al. [2]. In the author's opinion, the deformation of sample at the post-peak phase is non-homogeneous and the calculated values of the parameters α_3 and β_3 may not be correct. The value of error is unknown.

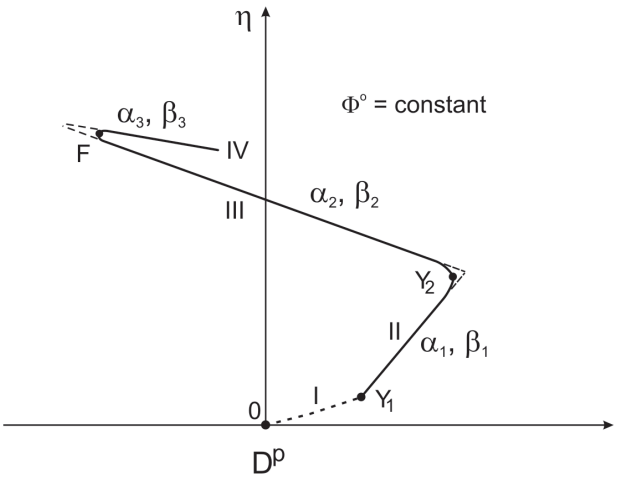

Figure 1: Scheme of stress ratio–plastic dilatancy relationship.

4 Calculation Methods And Results

Some experimental relations, such as q–ε_a, ε_υ–ε_a, published for ballast were sectionally approximated by higher-degree polynomials. Then, the increments of stress ($\delta p'$, δq) and strains ($\delta\varepsilon_\upsilon$, $\delta\varepsilon_q$) were calculated. For the assumed values of κ and ν (Tables 1 and 2), the plastic parts of the volumetric and shear strain increments were calculated. The η–D^p experimental relationship and the linear approximation for each stage of shearing were found. The approximately straight lines establish the values of the parameters: α_1, β_1, α_2, β_2, α_3 and β_3. Establishing an approximate value of Φ° for the ballast based only on data from some drained triaxial tests is difficult. In this paper, it is assumed that at Stage III of shearing, the ballast behaviour is almost purely frictional. For purely frictional behaviour, α=0 and β=1.0 [7]. The mean value of η for D^p=0 at Stage III is taken as the value of M°, and the value of angle Φ° was calculated using Eq. (2.d). It is assumed that Φ°=38.2° for scaled ballast and Φ°=41.0° for fouled ballast. These values are consistent with the findings of Indraratna and Salim [9]. The values of the secant shear modulus G_s were also calculated for the analysed experiments. The relationships q–ε_a, ε_υ–ε_a, G_s–ε_a, and η–D^p for scaled and fouled ballast are shown in Figures 2–5 respectively. Analysing the relationship η–D^p, the locations of the characteristic points were found and are shown in Figures 2–5.

The axial strains related to the characteristic points, namely, Y_1, Y_3 and F are summarised in Tables 3 and 4 for scaled and fouled ballasts, respectively. In Tables 3 and 4, the values of the parameters α and β are also shown.

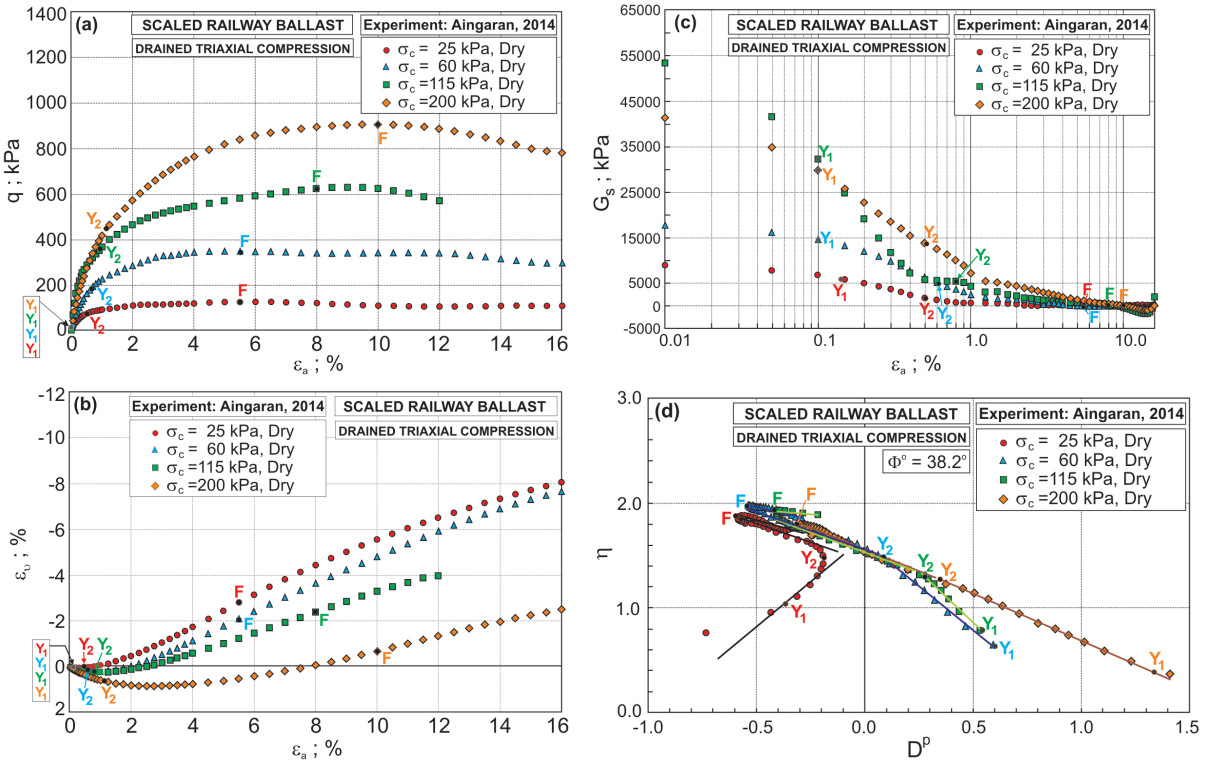

Figure 2: Relationships for dry scaled ballast: (a) q–ε_a; (b) ε_v–ε_a; (c) G_s–ε_a; and (d) η–D^p.

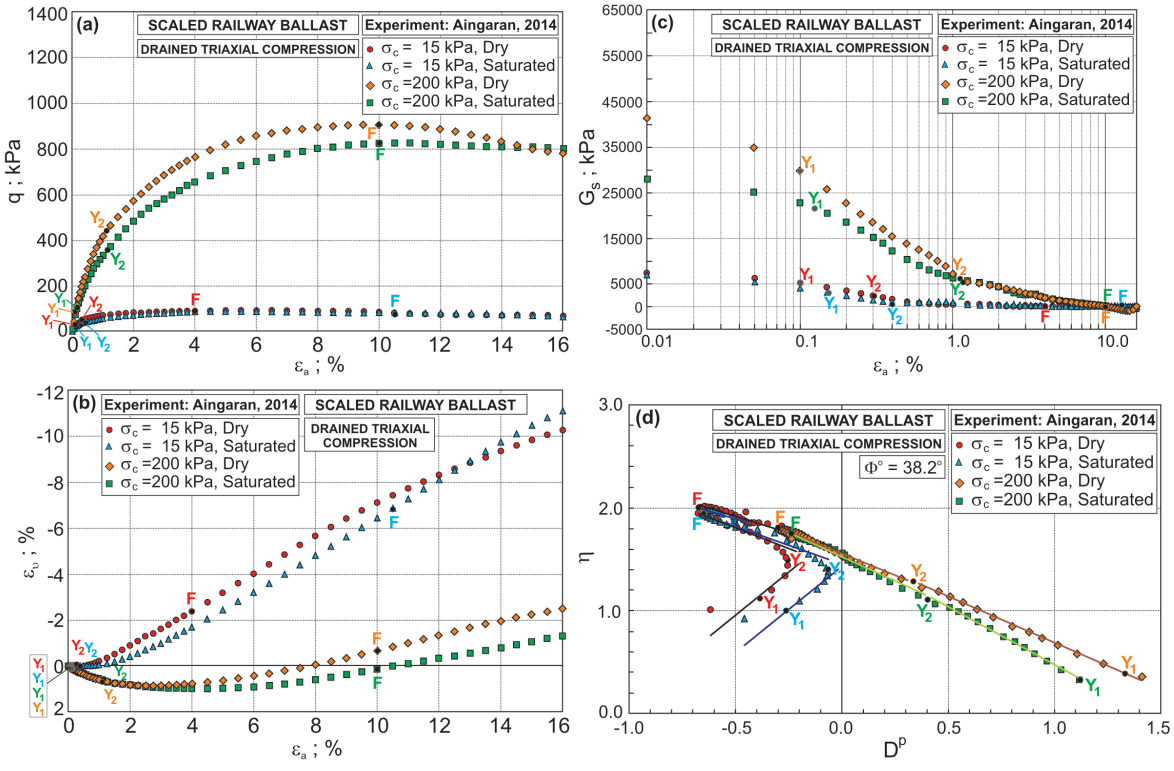

Figure 3: Relationships for saturated scaled ballast: (a) q–ε_a; (b) ε_v–ε_a; (c) G_s–ε_a; and (d) η–D^p.

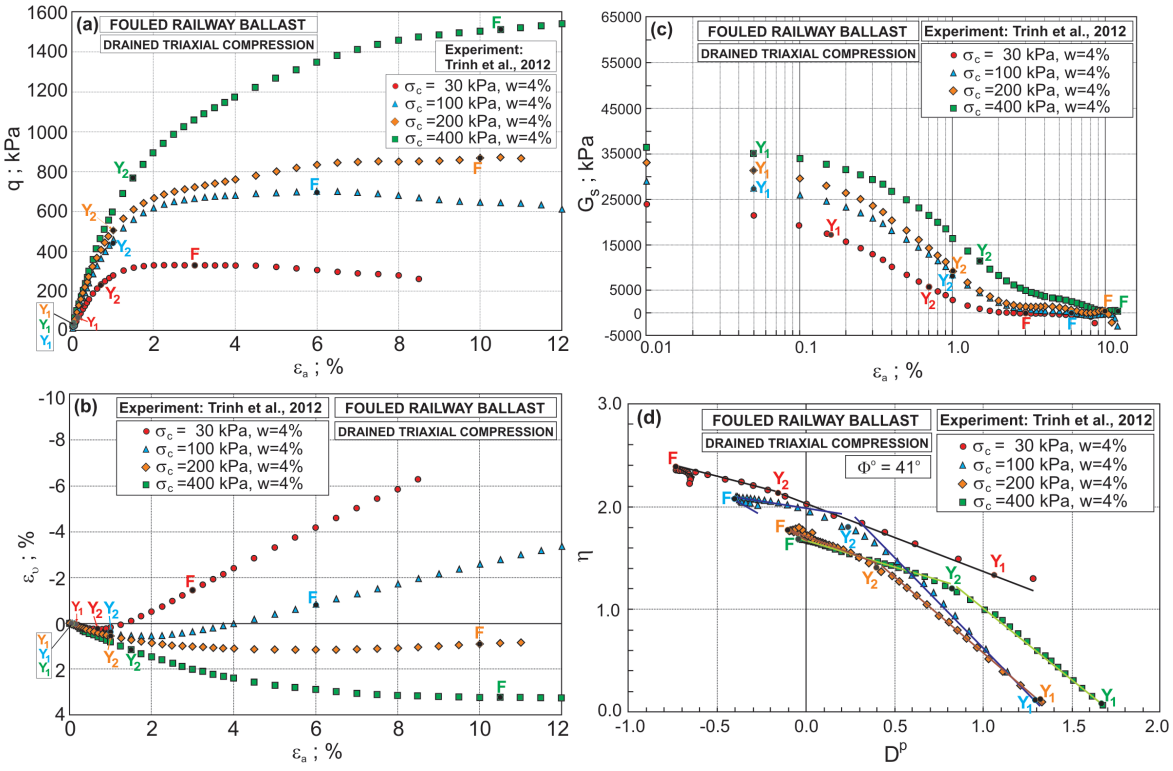

Figure 4: Relationships for fouled ballast at 4% water content: (a) q–ε_a; (b) ε_υ–ε_a; (c) G_s–ε_a; and (d) η–D^p.

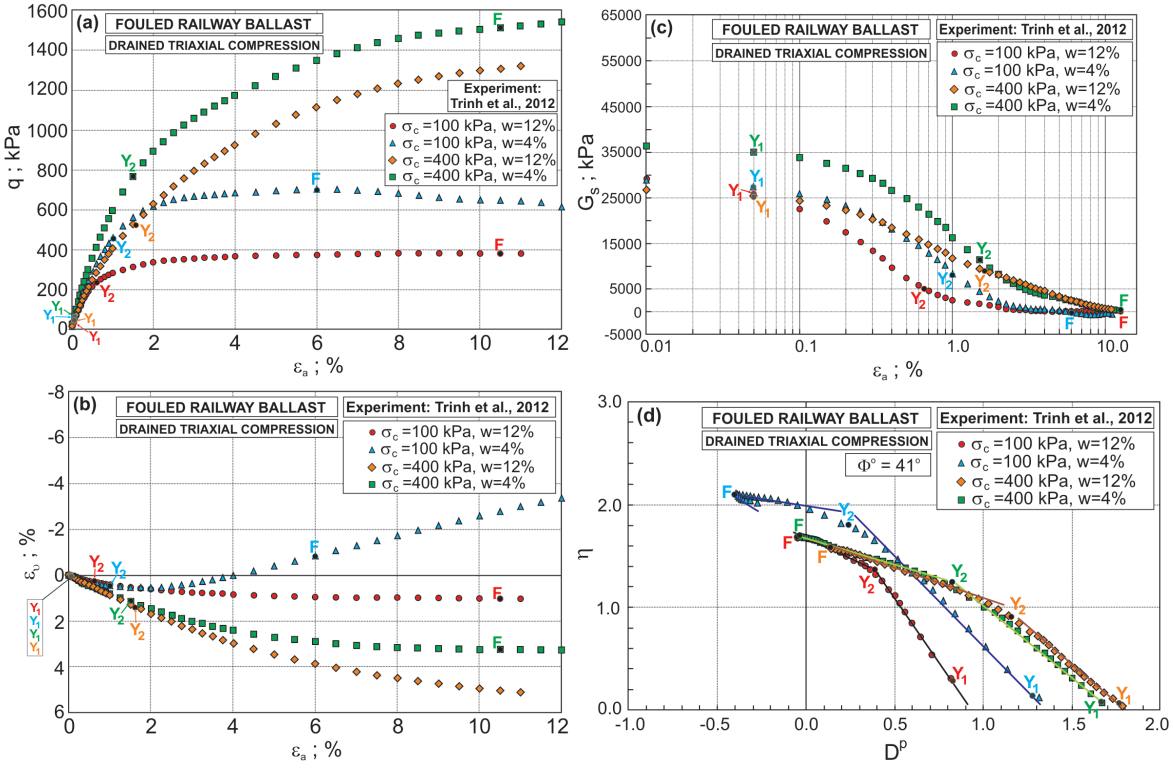

Figure 5: Relationships for fouled ballast at 4% and 12% water contents: (a) q–ε_a; (b) ε_υ–ε_a; (c) G_s–ε_a; and (d) η–D^p.

Table 3: Characteristic points and stress–dilatancy parameters for scaled railway ballast.

σ_c [kPa]	w	ε_a [%]			Parameters α and β					
		Y_1	Y_2	F	α_1	β_1	α_2	β_2	α_3	β_3
15	Dry	0.10	0.30	4.00	−0.70	−3.5	0.28	1.60	−0.10	1.30
25		0.15	0.50	5.50	−0.30	−3.5	0.22	1.50	0.00	1.20
60		0.10	0.60	5.50	−0.15	3.5	0.00	1.50	−0.35	1.00
115		0.10	0.90	8.00	−0.65	4.2	0.05	1.60	−0.63	0.30
200		0.10	1.1	10.00	−0.10	1.9	0.00	1.80	−0.00	1.80
15	Saturated	0.15	0.40	10.50	0.25	−3.5	0.20	1.50	−0.05	1.30
200		0.12	1.15	10.00	0.05	2.2	-0.15	2.05	0.00	1.50

Table 4: Characteristic points and stress–dilatancy parameters for fouled railway ballast.

σ_c [kPa]	w [%]	ε_a [%]			Parameters α and β					
		Y_1	Y_2	F	α_1	β_1	α_2	β_2	α_3	β_3
30	4.0	0.16	0.70	3.0	−0.80	1.50	−0.90	1.00	0.00	2.20
100	4.0	0.05	1.00	6.0	−1.60	4.00	−0.70	0.60	0.00	2.20
200	4.0	0.05	1.00	10.0	−0.90	3.40	−0.08	1.50	0.00	2.20
400	4.0	0.05	1.50	10.5	−1.70	3.20	0.00	1.20	0.00	1.20
100	12.0	0.05	0.65	10.5	−1.50	5.70	0.00	1.90	0.00	1.90
400	12.0	0.05	1.60	–	−2.30	3.40	0.00	1.30	–	–

It is simply visible that the characteristic points are very characteristic only in the η–D^p plane. In other planes: q–ε_a, ε_υ–ε_a and G_s–ε_a localisation of these points is not characteristic. So, the Frictional State Theory gives a new possibility for describing the mechanical behaviour of ballast. The behaviour of scaled and fouled ballasts is similar to that of latite basalt [10].

Elastic/quasi-elastic behaviour is observed at the initial stage of shearing, similar to the behaviour of some sands [11]. For high stress levels, plastic strains are observed almost at the start of shearing.

Parameters α and β represent the combined influence of grain crushing and rearrangement, the fault of experiment and the assumed procedure of approximation. By analysing only some drained triaxial compression tests within a narrow range of confining pressures, it is very difficult to properly establish all mechanical parameters of ballast.

5 Conclusions

The Frictional State Theory gives new possibilities for describing the mechanical behaviour of ballast.

Characteristic four stages of shearing are observed for almost all the analysed experiments.

At low stress level, the behaviour of ballast greatly differs from that at higher stress level due to the various possibilities of dilation at shearing.

In the author's opinion, the Frictional State Theory may be used for the modelling of ballast behaviour within the elasto-plasticity framework in the future.

More experimental and theoretical research is needed to fully confirm the usefulness of the Frictional State Theory for special soils such as ballast in the future.

Acknowledgement: This work, conducted at the Bialystok University of Technology, Poland, was supported by Polish Financial Resources on Science under project numbers S/WBiIS/6/2013 and S/WBiIS/2/2018.

References

[1] Aingaran, S. (2014). Experimental investigation of static and cyclic behaviour of scaled railway ballast and the effect of stress reversal. Ph.D. Thesis. Faculty of Engineering and Environment, University of Southampton.

[2] Trinh, V.N., Tang, A.M., Cui, Y.-J., Dupla, J.-C., Canon, I., Calon, N., et al. (2012). Mechanical characterization of the fouled ballast in ancient railway track substructure by large-scale triaxial tests. *Soils and Foundations, 52*(3), 511-523.
[3] Indraratna, B., Ionescu, D., Christie, H.D. (1998). Shear behaviour of railway ballast based on large-scale triaxial tests. *Journal of Geotechnical and Geoenvironmental Engineering, 124*, 439-450.
[4] Indraratna, B., Salim, W. (2001). Shear strength and degradation characteristics of railway ballast. In: *Proceeding of 14th Southeast Asian Geotechnical Conference*, Hong Kong, Balkema, Vol. 1, pp. 521-526.
[5] Werkmeister, S., Numrich, R., Dawson, A.R., Wellner, F. (2003). Design of granular pavement layers considering climatic conditions. *Transportation Research Record, 1837*, 61-70.
[6] Ekblad, J. (2006). Influence of water on coarse granular road material properties. *Road Materials and Pavement Design, 7*(3), 369-404.
[7] Szypcio, Z. (2016). Stress-dilatancy for soils. Part I: The frictional state theory. *Studia Geotechnica et Mechanica, 38*(4), 51-57.
[8] Szypcio, Z. (2016). Stress-dilatancy for soils. Part II: Experimental validation for triaxial tests. *Studia Geotechnica et Mechanica, 38*(4), 59-65.
[9] Indraratna, B., Salim, W. (2005). *Mechanics of Ballasted Rail Tracks: A Geotechnical Perspective*. Taylor & Francis Group, London.
[10] Dołżyk-Szypcio, K. (2018). Stress-dilatancy for crushed latite basalt. *Studia Geotechnica et Mechanica, 40*(1), 6-10.
[11] Coop, M.R., Willson, S.M. (2003). Behaviour of hydrocarbon reservoir sands and sandstones. *Journal of Geotechnical and Geoenvironmental Engineering*, ASCE, *129*(11), 1010-1019.